IEEE Access
Multidisciplinary | Rapid Review | Open Access Journal

Received 28 May 2024, accepted 11 June 2024, date of publication 14 June 2024, date of current version 22 August 2024.

Digital Object Identifier 10.1109/ACCESS.2024.3414966

RESEARCH ARTICLE

Optimizing the Transaction Latency in the Blockchain-Integrated Energy-Trading Platform in the Standalone Renewable Distributed Generation Arena

MARTIN ONYEKA OKOYE[1], (Member, IEEE), JUNYOU YANG[2], JIA CUI[2], AKHTAR HUSSAIN[3], (Member, IEEE), VAN-HAI BUI[4], (Member, IEEE), AND DANNY ESPIN-SARZOSA[5], (Member, IEEE)

[1]School of Electrical Engineering, Pontificia Universidad Católica de Valparaíso, Valparaíso 2374631, Chile
[2]School of Electrical Engineering, Shenyang University of Technology, Shenyang 110870, China
[3]Department of Electrical and Computer Engineering, University of Alberta, Edmonton, AB T6G 2R3, Canada
[4]Department of Electrical and Computer Engineering, University of Michigan–Dearborn, Dearborn, MI 48128, USA
[5]Departamento de Ingeniería Eléctrica, Universidad Técnica Federico Santa María, Valparaíso 2390123, Chile

Corresponding author: Martin Onyeka Okoye (martin.okoye@pucv.cl)

This work was supported in part by the Research Fund of the School of Electrical Engineering, Pontificia Universidad Católica de Valparaíso.

ABSTRACT Renewable distributed generations are associated with generation intermittency. Exacerbated by the consumption and demand uncertainty and their resulting mismatch, its energy trading suffers similar uncertainty. The situation is severe in the standalone distributed generations (SDG) for lacking transaction access to the utility grid. This paper proposes the energy transaction time determination and minimization algorithm for consumers in the SDG arena. First, blockchain technology is adopted for transaction enhancement and transaction data acquisition. The acquired blockchain data includes the hourly nodes (number of blockchain members), transaction sizes, and corresponding transaction durations. Next, the blockchain-recorded transaction data are fitted using the linear regression (LR) algorithm to obtain their fitting formula. The fitting formula was subsequently optimized in hourly intervals to obtain the optimal transaction time (energy delivery time) using particle swarm optimization (PSO). Finally, the optimal results are presented in a decision tree (DT) to energy consumers in the blockchain platform. Consequently, their transaction decision-making is guided by the result against the inherent transaction time uncertainty. Consumers can thus correctly adjust their transaction habits to suitably adapt to the transaction duration fluctuations in the energy trading arena. Energy transaction delays and transaction costs are consequently minimized leading to greater penetration of renewables and bridging the generation and consumption gap.

INDEX TERMS Blockchain technology, decision tree (DT), linear regression (LR), number of nodes, particle swarm optimization (PSO), peer-to-peer energy trading, standalone distributed generations (SDG), transaction size, transaction time.

NOMENCLATURE

Acronyms

BTC	Bitcoin.
DT	Decision Tree.
IDE	Integrated Development Environment.
LR	Linear Regresssion.
MG	Microgriid.
PSO	Particle Swarm Optimization.
P2P	Peer-to-Peer.
SDG	Standalone Distributed Generation.

Parameters

N	Number of nodes.

The associate editor coordinating the review of this manuscript and approving it for publication was Lei Chen.

T	Transaction time (Transaction latency).
Z	Block size.
t	Time interval.
N_x	Number of nodes at xth time interval.
T_x	Transaction time at xth time interval.
Z_x	Block size at xth time interval.
c_1, c_2	Acceleration coefficients of each particle.
I	Number of iterations.
P_b	Particle's local best position.
P_g	Particle's global best position.
P_b-X_i	Cognitive component of each particle.
P_g-X_i	Social component of each particle.
r_1, r_2	Random numbers.
r2 score	Coefficient of determination.
V_i	Initial velocity of each particle.
V_{i+1}	New velocity of each particle.
ω	Particle's weight of inertia.
ωV_i	Inertia component of each particle.
X_i	Particle's initial position.
X_{i+1}	Particle's new position.

I. INTRODUCTION

A. ENERGY AVAILABILITY IN THE STANDALONE DISTRIBUTED GENERATION ARENA

At each instance in the utility grid, the energy buying and selling prices are ideally given [1]. Grid-connected microgrids (MGs) and distributed generations uphold these prices in the energy transactions with the utility grid. This ideally implies that energy is available to the consumers at all times and at will. As a result, the utility grid steadily assists the grid-connected distributed generations in achieving supply reliability and availability timeliness [2]. When the utility grid is, however, located too far from consumers' locality, the grid remains unconnected due to the corresponding high cost of electricity transmission over a very long distance [3]. Also, even the grid-connected MGs become islanded when a fault of high magnitude is encountered in the main grid [4], [5]. This is to keep the consumers in the MG unaffected. During this time, energy consumption is dependent on the localized and distributed generation sourced as well as their availability timeliness. In standalone distributed generations (SDG), the grid-connected energy supply reliability and its availability timeliness benefits are however unobtainable. This leads to uncertainties in energy reliability and availability timeliness.

The blockchain is thus introduced to address this problem and enhance the peer-to-peer (P2P) energy transaction experience. Blockchain technology offers rapid transaction access and convenience in a peer-to-peer transaction association [6]. Originating from the financial sector, it was introduced in the distributed energy generation market to enhance the transaction methodology amongst energy prosumers and consumers. Other promising features of its adoption include [7] high security, transaction transparency, record-keeping of transaction details, etc. The blockchain, however, is associated with transaction time delay and its delay duration variability and uncertainty [8]. This is due to its limited transaction bandwidth [9].

B. BLOCKCHAIN TRANSACTION TIME LATENCY AND UNCERTAINTY

Transaction delays are experienced with blockchain technology for several reasons. First, each initiated transaction ideally goes through a two-step security check protocol before it is admitted [10], [11]. It is first verified by the miners. Secondly, the verified transaction is forwarded to the entire blockchain members for validation before it is finally admitted and added to the growing chain. However, in the verification process, due to the growing number of transactions, the first-step verification by miners is far more delayed during periods of high transaction traffic. Miners are individuals who are responsible for approving initiated blockchain transactions by solving a computational puzzle with high-end computers [12] Every approved transaction is stored in a transaction block until it is filled. The block is subsequently sent to the blockchain members for approval thereafter it is added to the chain. Thus, the total transaction delay is a drawback factor.

Furthermore, sometimes transactions get stuck in the mempool after a long period of delay in the transaction queue [13], [14]. This could eventually be reversed. In addition, in some circumstances, more than one transaction block might be approved concurrently during which only one block is normally allowed to be appended. Others, known as lossy blocks are not added leading to much more delays. This is such because only one block can be sent at a time. Meanwhile, each transaction block has a content size limit to pass through a given transaction bandwidth [15]. This restricts the total individual transactions to this size thus limiting the average transaction time. In addition, as a security measure, each transaction block has a minimum time duration that must be exhausted before it is added to the chain. For example, in Bitcoin, it is 10 minutes [16]. These collectively increase the transaction delays. Delays in energy purchase could propagate generation-load imbalance and the consequent power variations [17] resulting in fluctuations in voltage/frequency (V/F) [18].

Also, the cost of transactions is increased during periods of high transaction traffic [19]. The miners are basically paid from the reward attached to each block that is added to the chain by them [20]. Another source of payment to miners is transaction tokens that the consumers attach to each of their initiated transactions to earn higher priority during approval [21]. The higher the token received from a consumer the higher the chances of being attended to earlier. This is because miners want to earn higher tokens. Thus, during high transaction traffic, consumers append much higher tokens to their initiated transactions to earn higher priority. A higher transaction token during a low transaction traffic leads to the least transaction latency. Conversely, the maximum transaction latency is experienced when a low token is paid during

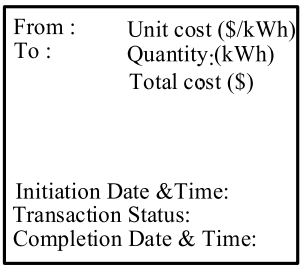

FIGURE 1. A sample of blockchain transaction record.

a high transaction traffic [22]. Consequently, such survival-of-the-fittest exercise amongst the energy traders leads to a high cost of energy transactions. Meanwhile, transaction reward on each block in some blockchains is designed to be reduced as more transactions take place or as time goes on. For instance, the transaction reward in Bitcoin is designed to be reduced to half every four years or every new 210,000 blocks [23], [24]. It was halved to 6.25 bitcoin (BTC) in the year 2020. Thus, it is expected to be 3.125 BTC in the year 2024 or at the creation of additional 210, 000 blocks, whichever comes first. Hence, miners would develop greater interest in the higher transaction tokens received from each transaction.

It was successfully established in our paper in [6] that blockchain transaction delay is directly affected by the growing transaction size and the *number of nodes*. The number of nodes is the number of blockchain members. Since their magnitude is uncertain at any point in time, the transaction time remains uncertain. It was adduced that transaction time is directly proportional to transaction size and the number of nodes. Thus, an equation can be obtained relating the three quantities. On the other hand, blockchain characteristically hosts a data record of each completed transaction [25], [26]. The record includes transaction size, the associated number of nodes, the transaction time duration, the address of the transactors, etc. Taking advantage of the blockchain transaction record-keeping feature, we propose a transaction time minimization approach. This is to increase transaction speed, reduce transaction costs (transaction fees), and foster greater integration of renewables. Consequently, the minimum values of transaction sizes and number of nodes can be obtained for each hourly interval.

C. RESEARCH CONTRIBUTIONS

Researchers have made substantial achievements in the effort to transaction time enhancement. Literature [6] proposed a blockchain-adopted method for transaction enhancement in peer-to-peer electricity trading. It however did not consider the optimization approach in the transaction time management. The transaction time manipulation approach was demonstrated in [8]. Consequently, a user-friendly method was proposed for comfortably deciding the consortium P2P transaction time in advance by adjusting the transaction size and number of members. However, a method to minimize

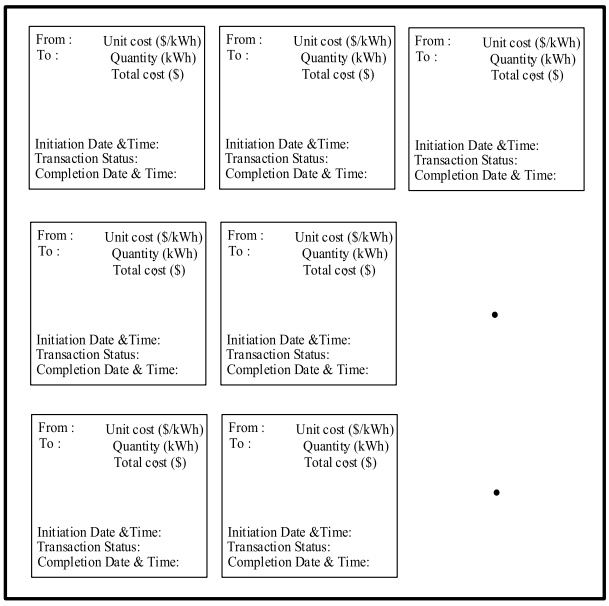

FIGURE 2. A blockchain transaction block.

the transaction time was not covered. A secure method of remote data transmission was successfully proposed in [27] using blockchain. However, a collective optimization of the transfer time is not within its scope. The real-time transaction time optimization and subsequent increase in the penetration of renewables however remained a necessity in the blockchain-integrated energy trading arena. This paper, thus, proposes a method for achieving P2P energy transactions at minimal delay. Consequently, the following contributions are made:

i. Blockchain technology is integrated into the energy-to-consumer platform to achieve enhanced, secure, and low-cost electrical energy accessibility to consumers in the SDG arena. Next, a relationship between the blockchain transaction time, transaction size, and the number of nodes is determined leading to real-time energy transaction duration awareness.
ii. Subsequently, the obtained relationship equation is optimized by minimizing the transaction time (transaction delay) in each hourly interval. This deciphered the transaction time fluctuation pattern.
iii. Finally, the optimized result is fitted and displayed on a decision tree (DT) for ease of accessibility. This presents hourly periods of low transaction time for the energy traders to take advantage of. Consequently, energy generation is made more available to consumers at minimal delay and minimal transaction cost.

II. ENERGY-TRADING ECOSYSTEM

A. DISTRIBUTED ENERGY SYSTEM

The distributed energy system is characterized by modular energy generations spanned over a range of distances along with individual storages. Depending on the climatic

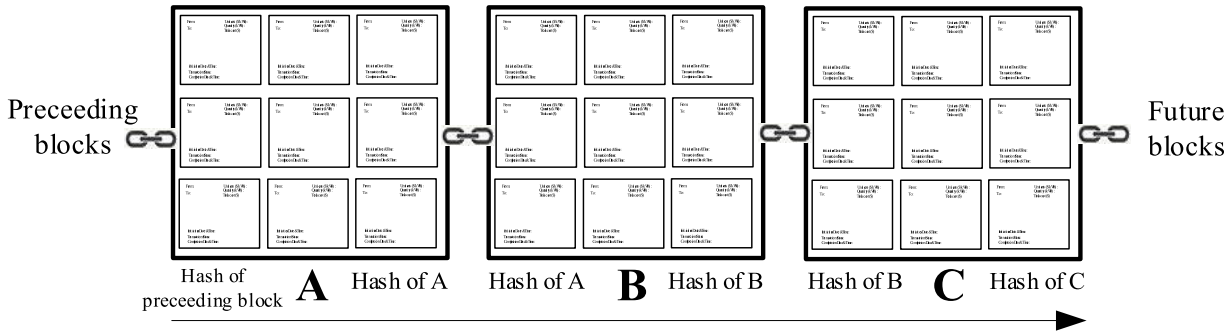

FIGURE 3. A blockchain transaction chain.

characteristics of the location, various generation sources are adopted with each environment taking advantage of its feature. For instance, photovoltaic generation is common in locations that are characterized by high peak sun hours (PSH). While some electricity users are non-generating consumers, some generate at insufficient capacities that do not surpass personal consumption requirements. Others generate in commercial quantity. Due to the variability of renewable sources and the energy characteristics of the SDG arena, producers tend to store the generated energy. The stored energy serves two major purposes. One is for future consumption and the other is for trading to achieve remuneration benefits. Hence, a dispatch mechanism is initiated through P2P energy trading. To enhance the ease with which the energy reaches the consumers during the trading process, blockchain technology is integrated into the trading system.

B. BLOCKCHAIN TECHNOLOGY IN ENERGY MARKET

Blockchain technology was adopted in the electrical engineering discipline from the financial sector [28]. It was introduced in the electrical energy-trading domain to enhance the ease with which the generated energy is dispatched and transacted amongst peers. Various breakthroughs have been achieved with the welcomed technology such as decentralized transaction architecture [29]. This eliminated the middleman bottleneck that is associated with the centralized architecture. Thus, members could initiate transactions directly with one another thereby achieving faster P2P transactions. Also, the detail of each completed transaction is stored on the network with a copy of it sent to each member. Hence, transparent transactions are promised [30]. Before the advent of blockchain, transactions were typically managed by a middleman intervention. This makes transaction associates remain dependent on the successful approval and processing of their submitted transaction requests. Thus, the effect of any delay or inefficiency with the middleman is transferred among the energy traders. With the decentralized feature of blockchain, such shortcoming is jettisoned. In addition to a reduced transaction time, greater transparency is realized as the members now transact directly with one another [31]. Furthermore, each completed transaction is tied to the immediate-preceding transaction using an alpha-numeric key [32]. Hence, before a transaction is successfully altered, the adversary must know the alpha-numeric keys of all completed transactions. This is almost impossible. Thus, a secured transaction architecture is upheld.

Also, blockchain's high-security feature accounts for the increased acceptability of the crypto. The sequence of transaction protocol that accounts for the high security in the blockchain is as follows:

i. Consumers initiate and send energy transaction requests to the energy producers/sellers or marketers as shown in Fig. 1.
ii. The requested transactions are subsequently sent to the miners for validation via a mechanism called the proof-of-work.
iii. The validated transactions are stored in a block by miners as shown in Fig. 2 until the block is filled to the maximum allowable limit in megabytes.
iv. The filled block is returned to blockchain nodes for validation for approval in a consensus mechanism.
v. The approved block is finally added to the chain by a high-security mechanism. This is as shown in Fig. 3 for block A, block B, and block C. In some cases, step iv might be truncated depending on the members-agreed protocol that is programmed in the smart contract in which case the block would directly be added to the chain.
vi. The blocks are added to the chain by digitally locking each added block to both the preceding block and the next block. Such a lock is achieved by an alphanumeric key known as *Hash* [33]. Consequently, each block contains two different hashes in which one is tied to the immediate preceding block and the other to the immediate next block [34]. By this means, the security of the blockchain network is guaranteed [35], [36].

III. METHODOLOGY OF SIMULATION

The simulation methodology involves three simulation steps, namely: *transaction time* simulation, optimization of results obtained from transaction time simulations, and fitting of the optimal results on a DT for ease of data visualization. To aid

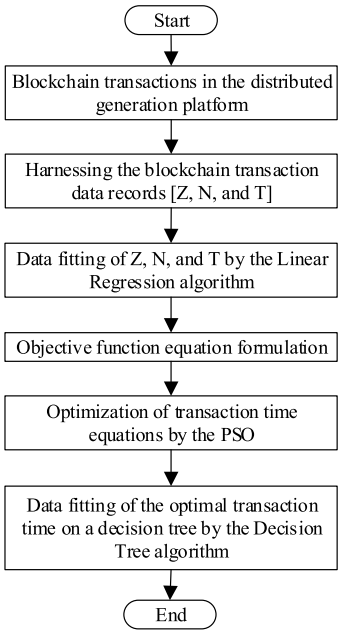

FIGURE 4. A flowchart of the research path and simulations.

comprehension, the path to the various simulations performed is given in the flowchart in Fig. 4. First, the linear regression (LR) algorithm is used to determine the relationship between the blockchain transaction block sizes, the number of nodes, and the transaction time.

A. TRANSACTION TIME SIMULATION

Transaction time simulation involves modeling the P2P transaction duration in the blockchain-integrated energy market. Three parameters were utilized namely: the transaction size (Z), the number of nodes (N), and transaction time (T). The transaction size (Z), also regarded as *block size*, is the size of completed transactions that were recorded at any given time interval. It is measured in kilobytes (KB). The number of nodes represents the number of registered blockchain members. Transaction time is the duration between when an energy transaction request is initiated to when the transaction is completed. Blockchain records its transaction details. Thus, the three data: T, Z, and N; can be obtained from the blockchain-recorded data.

1) TRANSACTION TIME DATA FORMULATION

To obtain the equation of the relationship between Z, N, and T, the blockchain transaction time data in our paper in [6] is considered. It was obtained using the network simulator 3 (NS3) to simulate the relative variations in the three quantities. NS3 is a network simulator for discrete events used in academic research to investigate how node-oriented network discrete quantities vary with one another. First, N was kept constant while Z was gradually increased from 10 KB to 3590 KB at the rate of 10 KB per step increment. The corresponding transaction time was measured and recorded in each increment. In the second phase, Z was kept constant

TABLE 1. Seed values for blockchain transaction time data generation.

Time interval, t	Seed value
2	10
3	11
4	12
5	13
6	14
7	15
8	16
9	17
10	18
11	19
12	20
13	21
14	22
15	23
16	24
17	25
18	26
19	27
20	28
21	29
22	30
23	31
24	32

while N was gradually increased from 2 to 500. Similarly, the corresponding values of T were recorded. In this paper, the data was required for 24-hour intervals. This is to represent the blockchain transaction time data for each hourly interval and be able to use the transaction time in each hour to make appropriate energy trading (buying and selling) decisions. Consequently, the existing one-hour data is emulated 23 times by generating them 23 times using a random number generator. This represents the remaining 23 hourly blockchain transaction time data. In the random number generation, the ranges of the entire 23 hourly data were maintained the same as those of the existing data. The range of the existing data for Z, N, and T are given in (1), (2), and (3), respectively.

$$10 \leq Z \leq 3590 \tag{1}$$

$$2 \leq N \leq 500 \tag{2}$$

$$0.86 \leq T \leq 115.16 \tag{3}$$

To enable the reproducibility of the simulation, a seed value is used for the random number generation in each of the 23 hours. This is to make the random values unchanging and thus regeneratable thereby enabling the reproducibility of our research paper simulations. The seed values that were used for the data generation in each of the hourly intervals are given in Table 1.

Fifteen random values were generated for each of Z, N, and T. This is to achieve an adequate quantity of data values with which the regression simulation would be performed to obtain the fitting formula on the data. The Z variable consists

```
1 import random
2 random.seed(10)
3 for i in range (15):
4     print(round(random.uniform(2, 500)))
```

FIGURE 5. Python code for N_2 data generation in the 2nd-hour interval.

```
1 import random
2 random.seed(32)
3 for i in range (15):
4     print(round(random.uniform(0.86, 115.16), 2))
```

FIGURE 6. Python code for T_24 data generation in the 24-hour interval.

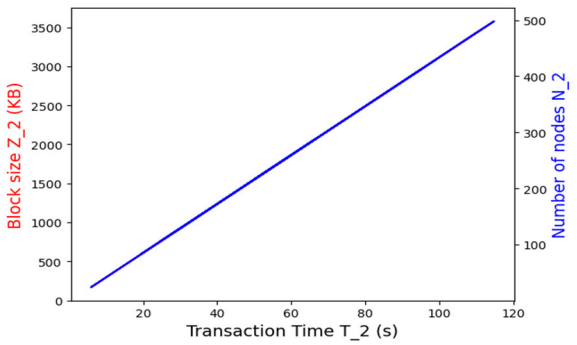

FIGURE 7. Data relationship between Z, N, and T in the 2nd-hour interval.

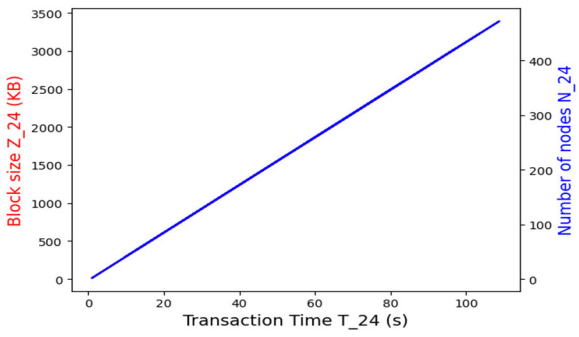

FIGURE 8. Data relationship between Z, N, and T in the 24th-hour interval.

of continuous values and is thus a 2-decimal *float*. This is because data transaction size in KB could assume decimal values. The N variable consists of discrete values since it represents the number of blockchain members. Hence they are positive integers. The T variable comprises 2-decimal *float* values. Thus, the random number generation adheres to these distinctive features of Z, N, and T variables. For example, the Python code for generating nodes (N_2) in the 2nd hour interval is given in Fig. 5 and the Python code for generating transaction time (T_24) in the 24th hour interval is given in Fig. 6. Line 2 generates the random data using the respective hour seed values given in Table 1. Line 3 generates the data in 15 samples. Line 4 prints the generated values within the data range stated in equations (2) and (3). For visualization purposes, the relationship in the generated transaction data (Z, N, and T) in interval 2 and interval 24 is given in Fig. 7 and Fig. 8, respectively. Subsequently, the data are fitted to obtain the fitting formula in each of the 24 hourly intervals.

2) TRANSACTION TIME SIMULATION AND EQUATION FORMULATION

To confirm the linearity of the obtained data, the data samples in the 2nd-hour interval (Z_2, N_2, T_2) and the 24th-hour interval (Z_24, N_24, T_24) were plotted. The graphs obtained are shown in Fig. 6 and Fig. 7, respectively. Following the linear relationship in the blockchain transaction time data, the LR algorithm was utilized to model the data and perform the simulation. Consequently, each of the data was divided into a 90% train set and a 10% test set in the Jupyter Notebook IDE of Python Programming language. The system information used for the simulations includes Dell running an operating system of Microsoft Windows 11 Pro with i5-12600K 3700 MHz processor, 32 GB RAM, and 1TB local disk storage. The selection of the test set was done by a random number seed of 90 (random_state = 90). This is to make the selected test data unchanging and the simulation reproducible. The regression accuracy metric, r2_score (coefficient of determination) on the test data, presented a value of 0.99 which is approximately 1. Zero is the least regressor prediction accuracy and 1 is the maximum accuracy. Subsequently, the individual 24 hourly fitting formulas obtained are presented in (4) ∼ (27). Each of the equations is in the form given in (28), where m_1 and m_2 are the slopes of the Z and N lines, respectively. k is the intercept of Z and N lines on the T axis, i.e., the value of T when the values of Z and N are zero.

$$T_1 = 0.012Z + 0.1393N + 1.23 \quad (4)$$
$$T_2 = 0.0315Z + 0.0028N + 0.5353 \quad (5)$$
$$T_3 = 0.0317Z + 0.0019N + 0.5397 \quad (6)$$
$$T_4 = 0.0317Z + 0.0015N + 0.5404 \quad (7)$$
$$T_5 = 0.0320Z + 0.0008N + 0.5410 \quad (8)$$
$$T_6 = 0.0321Z + 0.0015N + 0.5421 \quad (9)$$
$$T_7 = 0.0322Z + 0.0017N + 0.5412 \quad (10)$$
$$T_8 = 0.0314Z + 0.0039N + 0.5378 \quad (11)$$
$$T_9 = 0.0320Z + 0.0003N + 0.5389 \quad (12)$$
$$T_{10} = 0.0327Z + 0.0052N + 0.5440 \quad (13)$$
$$T_{11} = 0.0319Z + 0.0003N + 0.5373 \quad (14)$$
$$T_{12} = 0.0318Z + 0.0007N + 0.5410 \quad (15)$$
$$T_{13} = 0.0321Z + 0.0010N + 0.5392 \quad (16)$$
$$T_{14} = 0.0322Z + 0.0019N + 0.5419 \quad (17)$$
$$T_{15} = 0.0322Z + 0.0017N + 0.5387 \quad (18)$$
$$T_{16} = 0.0324Z + 0.0031N + 0.5446 \quad (19)$$
$$T_{17} = 0.0320Z + 0.0004N + 0.5432 \quad (20)$$
$$T_{18} = 0.0329Z + 0.0068N + 0.5440 \quad (21)$$
$$T_{19} = 0.0320Z + 0.0004N + 0.5399 \quad (22)$$
$$T_{20} = 0.0317Z + 0.0020N + 0.5386 \quad (23)$$

$$T_{21} = 0.0318Z + 0.0007N + 0.5425 \quad (24)$$
$$T_{22} = 0.0322Z + 0.0016N + 0.5407 \quad (25)$$
$$T_{23} = 0.0321Z + 0.0012N + 0.5401 \quad (26)$$
$$T_{24} = 0.0325Z + 0.0042N + 0.5465 \quad (27)$$
$$T = m_1 Z + m_2 N + k \quad (28)$$

B. TRANSACTION TIME OPTIMIZATION

To optimize the transaction time, (4) ∼ (27) are minimized in the 24 hourly intervals, respectively. Consequently, the format of the objective function of the optimization equation is given in (29) and the constraints are given in (30). The right-hand sides of (4) ∼ (27) are objective functions of the transaction time optimization which are subsequently optimized. The optimization simulation was performed in each of the 24 hourly intervals of the day.

$$\text{Min}\,[m_1 Z + m_2 N + k] \quad (29)$$
$$\left.\begin{matrix} Z^{\min} \le Z \le Z^{\max} \\ N^{\min} \le N \le N^{\max} \end{matrix}\right\} \quad (30)$$

To obtain the minimum transaction time in each time interval, each of the equations is optimized by minimization. Due to the heuristic characteristic of the transaction time dynamism in the blockchain trading platform, a search-based algorithm, the particle swarm optimization (PSO) algorithm, was utilized for the simulation. Consequently, the minimum transaction time T_1 to T_24 was achieved via optimizations of the objective functions in the 24 hourly intervals. To find the optimal converging point, search particles were deployed. The initial position of each particle is represented with X_i. In the search process, after each movement by each particle, the next position of each particle is updated as X_{i+1}. This is given in (31).

$$X_{i+1} = X_i + V_{i+1} \quad (31)$$

where V_{i+1} is the new velocity defined in (32).

$$V_{i+1} = wV_i + c_1 r_1 (P_b - X_i) + c_2 r_2 (P_g - X_i) \quad (32)$$

where w = particle's weight of inertia. It signifies the tendency of the particle to change its direction of swarm. V_i is the initial velocity of each particle. P_b is the local best position of each particle, P_g is the global best position amongst entire particles. c_1 and c_2 are the acceleration coefficients of each particle. c_1 is the tendency of a particle's movement to be influenced by its personal best solution. c_2 is the tendency of a particle's movement to be influenced by the global best solution, r_1 and r_2 are random numbers ranging from 0 to 1 with which the particles' positions are tuned for convergence. The random numbers, r_1 and r_2, were generated with a random seed of 30 to aid reproducibility of this simulation. wV_i is the inertia component of each particle, $(P_b - X_i)$ is the cognitive component of each particle, and $P_g - X_i$ is the social component of each particle. Other tuning parameters are n, w, c_1, c_2, and I, where n is the number of particles selected and I is the number of iterations performed in each simulation. Through iterations, the optimal number of particles was found to be 20.

IV. RESULTS AND ANALYSIS

A. TRANSACTION TIME OPTIMIZATION RESULTS AND ANALYSIS

In the simulation tuning process, several values of the tuning parameters were used in a bootstrapping process until the particles converged to a global optimum (minimum). This is the position where "all the $P_b = P_g$" within the given search space (minimum and maximum bounds). The values of the tuning parameters that were used to achieve convergence of the particles in the 2-head and 2-tail intervals are given in Table 2 along with the optimized results. The 2-head interval represents the first two hourly intervals (intervals 1 and 2) while the 2-tail interval is the last two hourly intervals (intervals 23 and 24). For sampling and data visualization purposes, the particles' swarm graphical positions in the 2-head and 2-tail intervals are given in Fig. 9 ∼ Fig. 12. The three various graphical positions of the 20 particles during the swarm movement in each of interval 1, interval 2, interval 23, and interval 24 are given in Fig. 9, Fig. 10, Fig. 11, and Fig. 12, respectively in the form of food-searching birds. It can be seen that the birds remained scattered in the first position of the swarm when the number of iterations was one. In the second position, the number of iterations was increased to three at each time hourly interval, and other tuning parameters were also readjusted. This got the birds closer to one another since they moved toward the lead bird whose position is P_b, i.e. the bird whose position is the closest to the food location. The lead bird is designated as the bird with the largest body size.

In the third position of the swarm, the search parameters were tuned further and the iteration was increased to 10. It was found at this point that all the birds in each hourly interval converged to a common position, P_b. This happened at the left bottom edge of the search space. It is circled in blue for easy identification. It is the position where the food lies. It is the position where the transaction time recorded an optimal value (minimum value). The optimal swarm position and the corresponding objective function value (transaction time) were obtained in each of the 24 hourly intervals and are approximately given in Table 3 and Table 4, respectively. This could also be done in a similar manner for each minute or second of the day, other than hourly intervals, leading to more precise transaction time information. However, an hourly interval was selected to reduce the complexity of the simulations and results.

Following the result obtained from the optimization simulation, it was observed that the data was nonlinear across the hourly time intervals (1∼24). This is as seen in Table 4. Hence, this necessitated the decision to model the result of the optimization using a non-linear model. The aim is to recognize the non-linear pattern in the data movement from time interval 1 ∼ 24 and obtain its fitting model. With the intent to graphically present the result on a DT for clarity,

TABLE 2. PSO tuning parameter and optimization results in the 2-head and 2-tail intervals.

Figure	Time interval, t	Swarm position	n	w	c_1	c_2	I	P_g (Z)	P_g (N)	T (f (Z, N))
9(a)	1	position 1	20	0.5	0.5	0.5	1	851.94618147	121.01521323	28.310773380208268
9(b)	1	position 2	20	0.5	0.8	0.8	3	884.8166466	2	11.595570891913514
9(c)	1	position 3	20	0.9	0.8	0.8	10	10	2	1.6286
10(a)	2	position 1	20	0.5	0.5	0.5	1	260.25009505	258.22668361	9.456212708039278
10(b)	2	position 2	20	0.5	0.8	0.8	3	169.51	258.81903795	8.085894946920448
10(c)	2	position 3	20	0.9	0.8	0.8	10	169.51	24	5.9420649999999995
11(a)	23	position 1	20	0.9	0.8	0.8	1	124.99966257	191.32932409	4.782184357567721
11(b)	23	position 2	20	0.9	0.8	0.8	3	53.96	177.89983508	2.5100856127074573
11(c)	23	position 3	20	0.9	0.8	0.8	10	53.96	8	2.281816
12(a)	24	position 1	20	0.9	0.8	0.8	1	102.64331334	234.25008713	4.866258049473514
12(b)	24	position 2	20	0.9	0.8	0.8	3	12.67	217.23698784	1.9788138487972162
12(c)	24	position 3	20	0.9	0.8	0.8	10	12.67	2	0.96

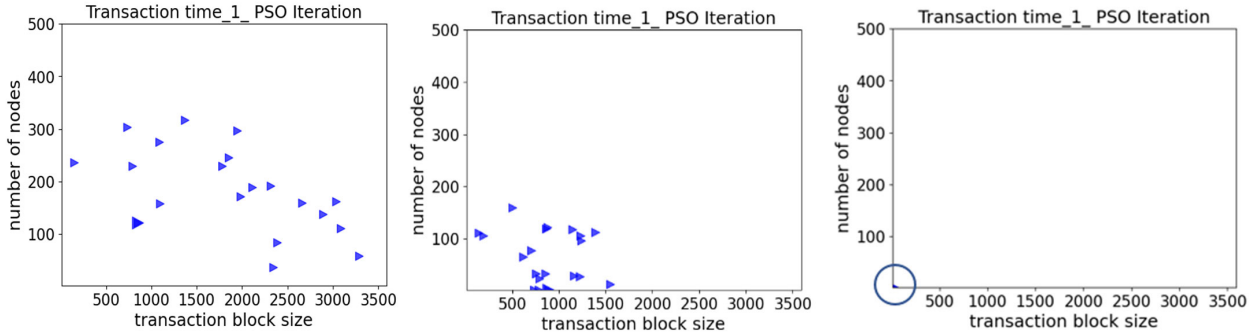

FIGURE 9. Positions of particles' swarm in the 1st-hour interval (a) iteration 1, (b) iteration 3, and (c) iteration 10 (convergence).

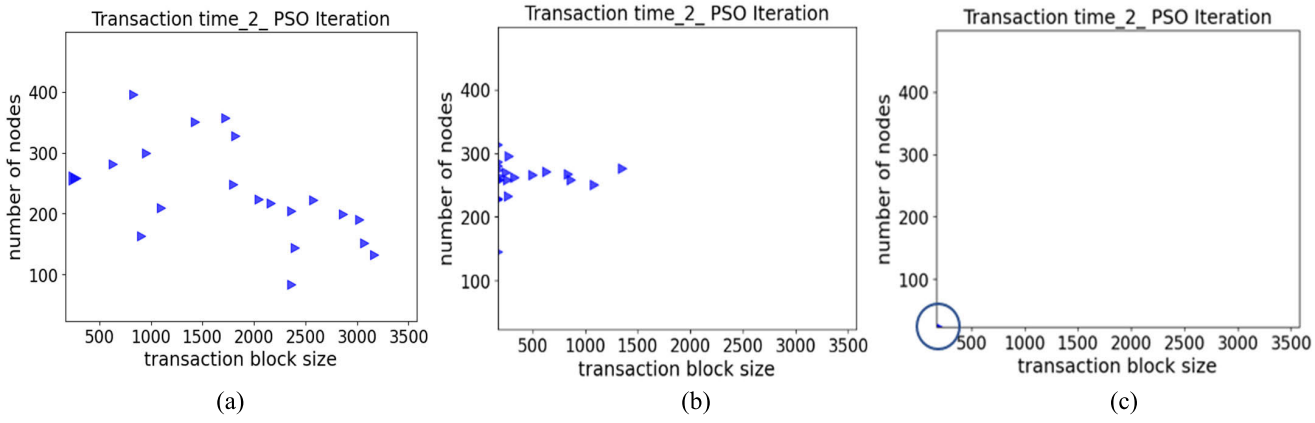

FIGURE 10. Positions of particles' swarm in the 2nd-hour interval (a) iteration 1, (b) iteration 3, and (c) iteration 10 (convergence).

the DT regressor, a nonlinear algorithm, was selected for the simulation.

B. DATA FITTING AND VISUALIZATION OF THE OPTIMIZED RESULTS

To enable easier visualization of the obtained results, the transaction time is displayed on the DT. For quick referencing, the magnitude of the transaction time is presented in a color band whose scale spans between white and orange. The white color represents the minimum transaction time and the orange color represents the maximum transaction time as shown in a scale in Fig. 13. Between the two extremes of the scale is the increasing or decreasing transaction time. Viewing the tree at any time, an observer can,

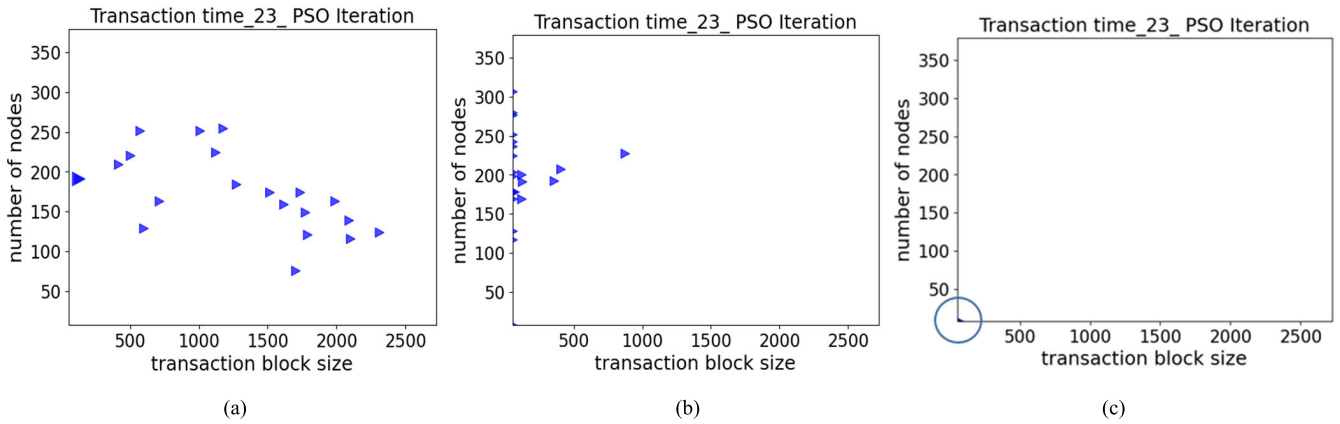

FIGURE 11. Positions of particles' swarm in the 23rd-hour interval (a) iteration 1, (b) iteration 3, and (c) iteration 10 (convergence).

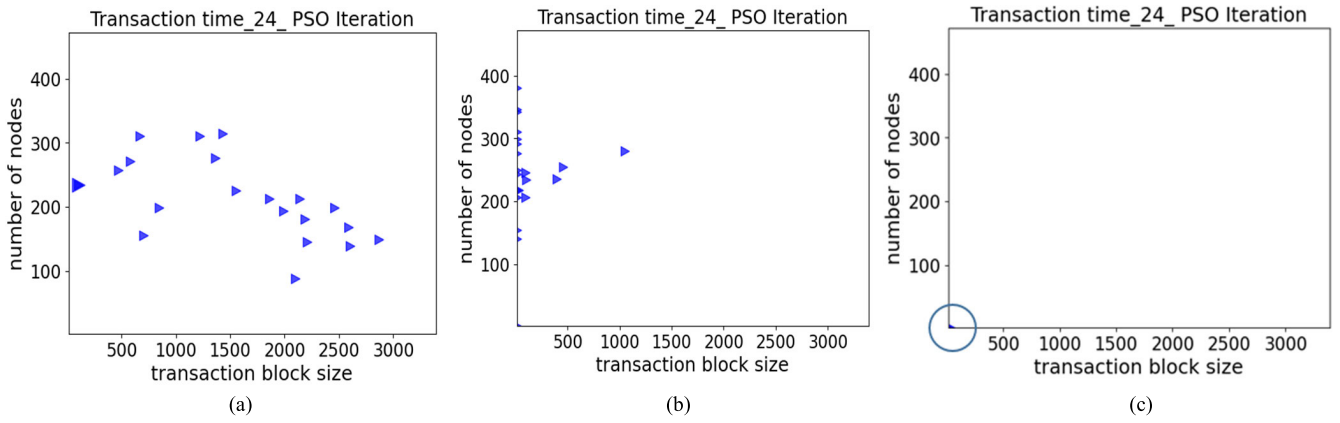

FIGURE 12. Positions of particles' swarm in the 24th-hour interval (a) iteration 1, (b) iteration 3, and (c) iteration 10 (convergence).

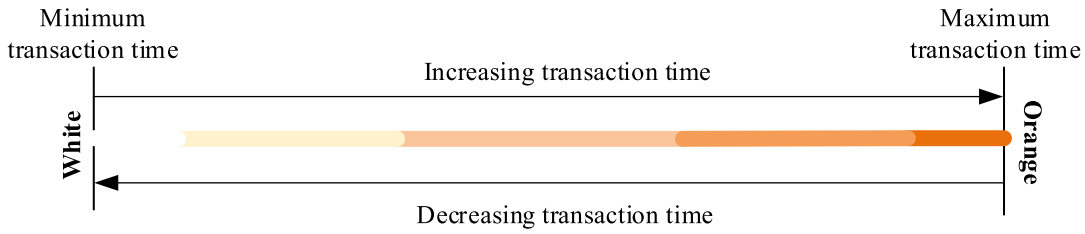

FIGURE 13. Transaction time alert notification color band.

thus, quickly identify the minimum or maximum transaction time at any moment in a matter of seconds based on the weight of the orange color. The lighter the orange color, the lower the transaction time, and vice versa. For instance, in the tree in Fig. 14, the minimum transaction time can easily be spotted by the whitish color in the middle right of the figure to be 0.96 seconds which took place at about a time interval that is greater than 23.5 hrs. This is exactly at 24:00 hrs in Table 4. Meanwhile, it is important to recall that 23.5 hrs is equivalent to 23:30 hrs in the ideal time scale. Similarly, the whitish color in the middle of the tree presented another very low transaction time of 1.22 seconds at about a time less than or equal to ($\leq$) 13:30 hrs. This was recorded at exactly 13:00 hrs. In comparison, the maximum transaction time can be spotted by the high weight of its orange coloration at about the middle of the figure to be 21.58 seconds. This occurred at about $\leq$ 10:30 hrs. In the tree, the first node at the topmost part is known as the root node. The last nodes that have no branches are known as the leaf nodes or terminal nodes. In between the root node and the leaf nodes are decision nodes that connect the root node to the leaf nodes. Each decision node has two sub-nodes. The information in the left side sub-node holds if the condition stated in its parent decision node is true. Otherwise, the information in the right side sub-node holds if

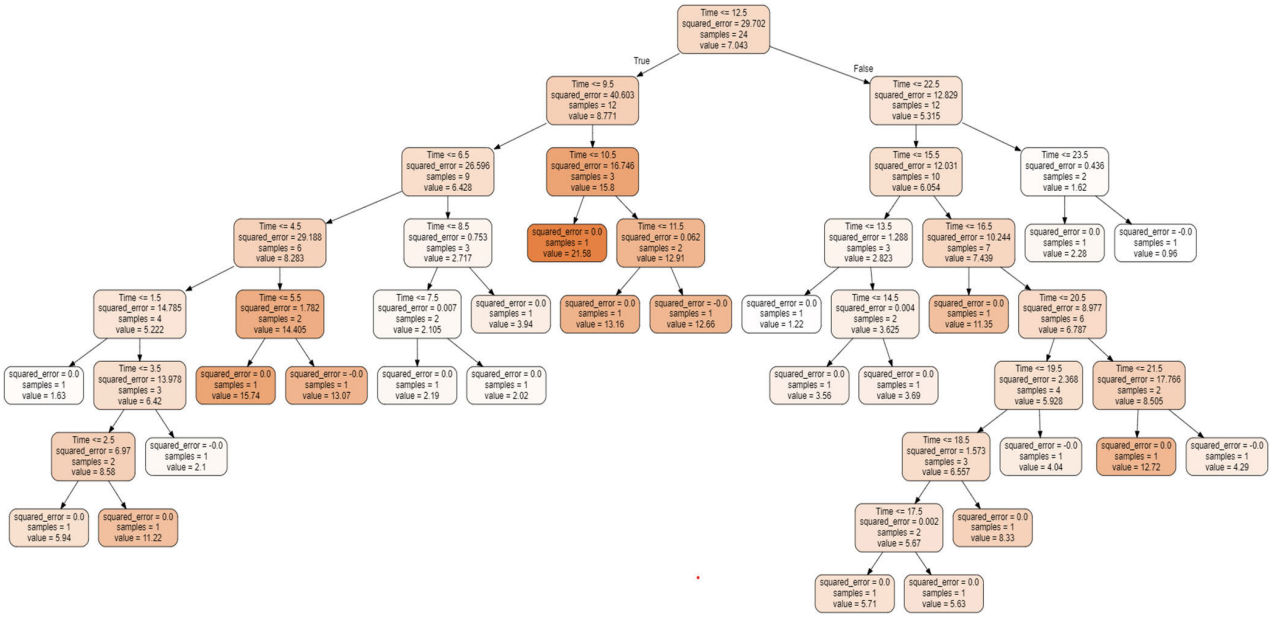

FIGURE 14. Data visualization of optimal transaction time on the decision tree.

TABLE 3. Optimal particles' positions in 24 hourly intervals.

Time interval (t)	Block size (Z	Number of nodes (N)	Transaction time (s)
1	10	2	1.63
2	169.51	24	5.94
3	334.6	47	11.22
4	48.88	7	2.1
5	476.16	67	15.74
6	392.45	55	13.07
7	51.72	8	2.19
8	46.26	7	2.02
9	106.43	15	3.94
10	658.93	92	21.58
11	395.37	56	13.16
12	379.63	53	12.66
13	21.39	4	1.22
14	94.55	14	3.56
15	98.67	14	3.69
16	338.6	48	11.35
17	161.76	23	5.71
18	159.42	23	5.63
19	244.02	35	8.33
20	109.51	16	4.04
21	381.36	54	12.72
22	117.53	17	4.29
23	53.96	8	2.28
24	12.67	2	0.96

TABLE 4. Optimal transaction time in 24 hourly intervals.

Time interval (t)	Transaction time (s)
1	1.63
2	5.94
3	11.22
4	2.1
5	15.74
6	13.07
7	2.19
8	2.02
9	3.94
10	21.58
11	13.16
12	12.66
13	1.22
14	3.56
15	3.69
16	11.35
17	5.71
18	5.63
19	8.33
20	4.04
21	12.72
22	4.29
23	2.28
24	0.96

the condition stated in its parent decision node is false. Also the same goes for the root node's immediate subnodes as it is seen stated.

It is important to recall that the specific uncertainties considered in this simulation process are the stochasticity in the transaction block size and the number of nodes, Thus, as the transactions proceed, these quantities change and the scale color is updated by the changing transaction values (transaction size, number of nodes, and their corresponding transaction time). Thus, the corresponding color weights would keep being updated for rapid identification of the periods of very low transaction time. During this time, a general reminder notification could be dispatched to all members to encourage more transactions. Similarly, a warning notification may be sent in vice versa. A notification alarm system could be triggered in addition to the color notification during the very low transaction time signals. The most important

TABLE 5. Comparison of our methodology with other works.

S/No	Features	Recent works	Our work
1	P2P transaction time	Determination	Determination and minimization
2	Result presentation	Numerical	Decision tree
3	Transaction time identification method	Numerical	Numerical and by color weights
4	Minimum transaction time update	At intervals	Dynamic by model simulation

highlight of the proposed approach is interdependency and synergy in the simulation steps that result in a dynamic update in the displayed results as the input data stochastically varies. This ranges from data capturing, down to data regression and optimizations and finally data fitting, all interconnected in functionality.

V. CONCLUSION

With the convenience of knowing the transaction situation from the comfort of electricity consumers' domicile, a more articulated trading decision can be reached. From the transaction time optimization simulations, the minimum transaction time was found to be 0.96 seconds. This occurred at 24:00 hrs. Consequently, the peaks in the transaction time can be more easily leveled. That is, transactions can be comfortably shifted to the hours when the transaction duration is at a minimum. This is achieved through the consumers' adaptive trading responses to the changing transaction time. In addition to the relieved stress and increased trading convenience, the consumers achieve a reduced trading cost. The usual extra charges levied on interested consumers at high-traffic hours by miners for quicker transaction services are eliminated. The chances of shedding critical loads due to the supply shortage caused by delayed transactions are minimized. In sole producers and prosumers, generations can thus be more correctly matched to the consumptions. Since the initiated transactions are now smoothly completed, energy producers can more accurately predict energy consumption linearly. This effect collectively bridges the gap between generation and consumption and realizes higher and more rapid penetration of renewables. This achievement could be proposed to the utility grid company as a method to tune down generations from fossil sources as the penetration of renewables increases. We opine that future research would be about methods to realize rapid renewable generations through weather forecasts so that new energy generations would match the various demand magnitudes made as a result of successful transaction time minimization and transaction cost minimization. The aim is to jettison the fossil sources and embrace a pollution-free generation.

REFERENCES

[1] A. Y. Ali, A. Hussain, J.-W. Baek, and H.-M. Kim, "Optimal operation of networked microgrids for enhancing resilience using mobile electric vehicles," *Energies*, vol. 14, no. 1, p. 142, Dec. 2020.

[2] M. Gholami, S. A. Mousavi, and S. M. Muyeen, "Enhanced microgrid reliability through optimal battery energy storage system type and sizing," *IEEE Access*, vol. 11, pp. 62733–62743, 2023.

[3] T. Boonraksa, W. Pinthurat, P. Wongdet, P. Boonraksa, B. Marungsri, and B. Hredzak, "Optimal capacity and cost analysis of hybrid energy storage system in standalone DC microgrid," *IEEE Access*, vol. 11, pp. 65496–65506, 2023.

[4] F. Zainab, K. Naz, K. K. Mehmood, S. B. A. Bukhari, A. Wadood, H. A. Khalid, and H. Park, "An optimal joint planning of DGs and electric vehicle charging stations in grid-connected and islanded microgrids," *IET Renew. Power Gener.*, vol. 17, no. 7, pp. 1623–1634, May 2023.

[5] T. E. Sati, M. A. Azzouz, and M. F. Shaaban, "Harmonic dual-setting directional overcurrent protection for inverter-based islanded microgrids," *IEEE Access*, vol. 11, pp. 34630–34642, 2023.

[6] M. Onyeka Okoye, J. Yang, J. Cui, Z. Lei, J. Yuan, H. Wang, H. Ji, J. Feng, and C. Ezeh, "A blockchain-enhanced transaction model for microgrid energy trading," *IEEE Access*, vol. 8, pp. 143777–143786, 2020.

[7] T. Vaiyapuri, K. Shankar, S. Rajendran, S. Kumar, S. Acharya, and H. Kim, "Blockchain assisted data edge verification with consensus algorithm for machine learning assisted IoT," *IEEE Access*, vol. 11, pp. 55370–55379, 2023.

[8] M. O. Okoye and H.-M. Kim, "Optimized user-friendly transaction time management in the blockchain distributed energy market," *IEEE Access*, vol. 10, pp. 34731–34742, 2022.

[9] X. Xie, C. Hua, J. Hong, P. Gu, and W. Xu, "AirCon: Over-the-air consensus for wireless blockchain networks," *IEEE Trans. Mobile Comput.*, vol. 23, no. 5, pp. 4566–4582, Jul. 2023.

[10] D. Das, S. Banerjee, P. Chatterjee, U. Ghosh, and U. Biswas, "Blockchain for intelligent transportation systems: Applications, challenges, and opportunities," *IEEE Internet Things J.*, vol. 10, no. 21, pp. 18961–18970, Nov. 2023.

[11] A. K. Yadav, K. Singh, A. H. Amin, L. Almutairi, T. R. Alsenani, and A. Ahmadian, "A comparative study on consensus mechanism with security threats and future scopes: Blockchain," *Comput. Commun.*, vol. 201, pp. 102–115, Mar. 2023.

[12] V. Ali, A. A. Norman, and S. R. B. Azzuhri, "Characteristics of blockchain and its relationship with trust," *IEEE Access*, vol. 11, pp. 15364–15374, 2023.

[13] G. Kaur, A. H. Lashkari, I. Sharafaldin, and Z. H. Lashkari, "Smart contracts and DeFi security and threats," in *Understanding Cybersecurity Management in Decentralized Finance: Challenges, Strategies, and Trends*. Cham, Switzerland: Springer, Jan. 2023, pp. 91–111. [Online]. Available: https://link.springer.com/chapter/10.1007/978-3-031-23340-1_5#citeas

[14] L. Besançon, C. F. Da Silva, P. Ghodous, and J.-P. Gelas, "A blockchain ontology for DApps development," *IEEE Access*, vol. 10, pp. 49905–49933, 2022.

[15] N. Mansoor, K. F. Antora, P. Deb, T. A. Arman, A. A. Manaf, and M. Zareei, "A review of blockchain approaches for KYC," *IEEE Access*, vol. 11, pp. 121013–121042, 2023.

[16] W. Zhao, I. M. Aldyaflah, P. Gangwani, S. Joshi, H. Upadhyay, and L. Lagos, "A blockchain-facilitated secure sensing data processing and logging system," *IEEE Access*, vol. 11, pp. 21712–21728, 2023.

[17] R. Sepehrzad, A. Mahmoodi, S. Y. Ghalebi, A. R. Moridi, and A. R. Seifi, "Intelligent hierarchical energy and power management to control the voltage and frequency of micro-grids based on power uncertainties and communication latency," *Electr. Power Syst. Res.*, vol. 202, Jan. 2022, Art. no. 107567.

[18] R. Sepehrzad, A. Hedayatnia, M. Amohadi, J. Ghafourian, A. Al-Durra, and A. Anvari-Moghaddam, "Two-stage experimental intelligent dynamic energy management of microgrid in smart cities based on demand response programs and energy storage system participation," *Int. J. Electr. Power Energy Syst.*, vol. 155, Jan. 2024, Art. no. 109613.

[19] J. Li, Y. Yuan, S. Wang, and F.-Y. Wang, "Transaction queuing game in Bitcoin BlockChain," in *Proc. IEEE Intell. Vehicles Symp. (IV)*, Jun. 2018, pp. 114–119.

[20] M. Hajiaghapour-Moghimi, E. Hajipour, K. A. Hosseini, M. Tavakkoli, S. Fattaheian-Dehkordi, M. Vakilian, and M. Lehtonen, "Hedging investments of grid-connected PV-BESS in buildings using cryptocurrency mining: A case study in Finland," *IEEE Access*, vol. 11, pp. 66327–66345, 2023.

[21] S. Islam, M. J. Islam, M. Hossain, S. Noor, K.-S. Kwak, and S. M. R. Islam, "A survey on consensus algorithms in blockchain-based applications: Architecture, taxonomy, and operational issues," *IEEE Access*, vol. 11, pp. 39066–39082, 2023.

[22] A. Battah, K. Salah, R. Jayaraman, I. Yaqoob, and A. Khalil, "Using blockchain for enabling transparent, traceable, and trusted university ranking systems," *IEEE Access*, vol. 11, pp. 23792–23807, 2023.
[23] M. Nour, J. P. Chaves-Ávila, and Á. Sánchez-Miralles, "Review of blockchain potential applications in the electricity sector and challenges for large scale adoption," *IEEE Access*, vol. 10, pp. 47384–47418, 2022.
[24] M. Wendl, M. H. Doan, and R. Sassen, "The environmental impact of cryptocurrencies using proof of work and proof of stake consensus algorithms: A systematic review," *J. Environ. Manage.*, vol. 326, Jan. 2023, Art. no. 116530.
[25] L. D. Costa, B. Pinheiro, W. Cordeiro, R. Araújo, and A. Abelém, "Sec-health: A blockchain-based protocol for securing health records," *IEEE Access*, vol. 11, pp. 16605–16620, 2023.
[26] A. Sasikumar, L. Ravi, K. Kotecha, A. Abraham, M. Devarajan, and S. Vairavasundaram, "A secure big data storage framework based on blockchain consensus mechanism with flexible finality," *IEEE Access*, vol. 11, pp. 56712–56725, 2023.
[27] B. Sharmila and T. K. Devi, "Theil–Sen regressive Miyaguchi–Preneel-based cryptographic hash blockchain for secure data transmission using remote sensing data in IoT," *IETE J. Res.*, vol. 70, pp. 116–129, Apr. 2023.
[28] H. U. Khan, M. Z. Malik, S. Nazir, and F. Khan, "Utilizing bio metric system for enhancing cyber security in banking sector: A systematic analysis," *IEEE Access*, vol. 11, pp. 80181–80198, 2023.
[29] M. H. D. Khan, J. Imtiaz, and M. N. U. Islam, "A blockchain based secure decentralized transaction system for energy trading in microgrids," *IEEE Access*, vol. 11, pp. 47236–47257, 2023.
[30] A. E. Bekkali, M. Essaaidi, and M. Boulmalf, "A blockchain-based architecture and framework for cybersecure smart cities," *IEEE Access*, vol. 11, pp. 76359–76370, 2023.
[31] S. Fugkeaw, "Achieving decentralized and dynamic SSO-identity access management system for multi-application outsourced in cloud," *IEEE Access*, vol. 11, pp. 25480–25491, 2023.
[32] A. Singh, R. A. Ikuesan, and H. Venter, "Secure storage model for digital forensic readiness," *IEEE Access*, vol. 10, pp. 19469–19480, 2022.
[33] P. M. Rao, S. Jangirala, S. Pedada, A. K. Das, and Y. Park, "Blockchain integration for IoT-enabled V2X communications: A comprehensive survey, security issues and challenges," *IEEE Access*, vol. 11, pp. 54476–54494, 2023.
[34] V. Malik, R. Mittal, D. Mavaluru, B. R. Narapureddy, S. B. Goyal, R. J. Martin, K. Srinivasan, and A. Mittal, "Building a secure platform for digital governance interoperability and data exchange using blockchain and deep learning-based frameworks," *IEEE Access*, vol. 11, pp. 70110–70131, 2023.
[35] M. Abdelsalam, M. Shokry, and A. M. Idrees, "A proposed model for improving the reliability of online exam results using blockchain," *IEEE Access*, vol. 12, pp. 7719–7733, 2024.
[36] J. Gomes, S. Khan, and D. Svetinovic, "Fortifying the blockchain: A systematic review and classification of post-quantum consensus solutions for enhanced security and resilience," *IEEE Access*, vol. 11, pp. 74088–74100, 2023.

MARTIN ONYEKA OKOYE (Member, IEEE) received the B.Eng. degree in electrical/electronic and computer engineering from Nnamdi Azikiwe University, Nigeria, in 2008, the M.Sc. degree in electronic systems design engineering from Universiti Sains Malaysia, Penang, Malaysia, in 2018, and the Ph.D. degree in electrical engineering from Shenyang University of Technology, Shenyang, China, in 2021. He was a Postdoctoral Researcher with the Department of Electrical Engineering, Incheon National University, Incheon, South Korea, until December 2022. He is currently a Profesor Asociado with the Department of Electrical Engineering, Pontificia Universidad Católica de Valparaíso, Chile. His research interests include generation system reliability assessment, blockchain technology, distributed renewable generations, and microgrid operation.

JUNYOU YANG received the B.Eng. degree from Jilin University of Technology, Jilin, China, the M.Sc. degree from Shenyang University of Technology, Shenyang, China, and the Ph.D. degree from Harbin Institute of Technology, Harbin, China. He was a Visiting Scholar with the Department of Electrical Engineering and Computer Science, University of Toronto, Canada, from 1999 to 2000. He is currently the Head of the School of Electrical Engineering, Shenyang University of Technology, China. He is also a Distinguished Professor of Liaoning province and the first hundred level candidates in the BaiQianWan Talents Program. He has led more than 50 research projects and has more than 200 publications in his technical field. His research interests include wind energy, special motor, and its control.

JIA CUI was born in 1987. He is currently a Postdoctoral Researcher, an Associate Professor, and the Departmental Leader of renewable energy science and engineering. His research interests include analysis and operation of smart grids, intelligent control, modeling and prediction of flexible load in distribution networks, and energy management technology of microgrids.

AKHTAR HUSSAIN (Member, IEEE) received the B.E. degree in telecommunications engineering from the National University of Sciences and Technology (NUST), Pakistan, in 2011, the M.S. degree in electrical engineering from Myongji University, Yongin, South Korea, in 2014, and the Ph.D. degree from Incheon National University, South Korea, in 2019. He is currently a Postdoctoral Fellow with the University of Alberta, Edmonton, Canada. His research interests include power system automation, smart grids, and microgrid operation.

VAN-HAI BUI (Member, IEEE) received the B.S. degree in electrical engineering from Hanoi University of Science and Technology, Vietnam, in 2013, and the Ph.D. degree in electrical engineering from Incheon National University, South Korea, in 2020. He was an Assistant Professor with the Department of Electrical Engineering, The State University of New York (SUNY) Maritime College, USA, from 2022 to 2023. Since August 2023, he has been appointed as an Assistant Professor with the Department of Electrical and Computer Engineering, University of Michigan–Dearborn, USA. His research interests include energy management systems, applications of machine learning in smart grids, and operation and control of power and energy systems.

DANNY ESPIN-SARZOSA (Member, IEEE) was born in Latacunga, Ecuador. He received the Electromechanics Engineering degree from the Universidad de las Fuerzas Armadas–ESPE, Ecuador, and the Ph.D. degree from the University of Chile. He is currently a Professor with the Department of Electrical Engineering, Universidad Técnica Federico Santa María, and a Research Associate with the Energy Center, FCFM, University of Chile. His research interests include load modeling, operation and planning of microgrids, renewable energies, decentralized energy solutions, and the development of solar-based small/medium size rural productive processes.